Dynamic Corrections of Object Motion Under the Influence of Self Motion

Ji-Ze Jang*^, Arya Khanal*, Yihe Chen, Kepler Palacio-Soto,
Gregory C. DeAngelis, and Ralf M. Haefner

Department of Brain & Cognitive Sciences, University of Rochester, Rochester, NY 14627, USA

Abstract

Vision is central to our ability to navigate the world. A problem of particular importance is how the brain estimates object motion during forward translation of an observer. To address this question, we tested the *flow parsing hypothesis*, which states that the brain uses structured patterns of retinal motion (*optic flow*) to infer self-motion, then subtracts the inferred self-motion from the retinal motion to estimate scene-relative motion of independently moving objects in the world (Warren and Rushton, 2008). We replicated Warren and Rushton (2009) to investigate mechanisms of flow parsing in two experiments using a 3D optic flow stimulus with stationary observers. Experiment 1 examined the effect of flow parsing when optic flow was present in the vicinity of the moving object (i.e., local) or further away from the object (i.e., global). We found that increasing global optic flow information in the visual field resulted in a greater degree of flow parsing (i.e., *relative tilt*). While the results are broadly consistent with those of Warren and Rushton (2009), they did not reach statistical significance most likely due to limited data. Experiment 2 examined the transferability of flow parsing across the visual field. Our findings are again consistent with those of Warrant and Rushton (2009), showing that relative tilt increases with distance from the fovea and persists when optic flow is confined to the hemifield opposite the moving object. However, the increase in relative tilt was again not statistically significant. The fact that our replication results were not statistically significant in either experiment likely reflects a lack of statistical power, and could be overcome by collecting more data from subjects. Finally, we extended Warren and Rushton (2009) by investigating whether the strength of flow parsing is tailored to the natural statistics of optic flow in the lower visual field. Prior research has shown that optic flow in the lower hemifield has a larger effect on subjects' heading responses than optic flow in the upper hemifield (Fujimoto & Ashida, 2019). Therefore, we expect to see a larger effect of flow parsing in the lower hemifield than in the upper hemifield in our on-going study.

---

* Equal contribution
^ Revisions to the original technical report by Ji-Ze Jang

Introduction

Myriad computations occur between the time light reaches the retina and the time by which the brain generates a cogent percept of our environment. One problem of particular importance is the estimation of scene-relative object motion during self movement. For instance, a stationary observer with normal vision perceives a vertically falling object as moving straight downward. On the other hand, when an observer is moving forward, the retinal motion of the object is altered by the ego movement. The brain of a forward-moving observer must first distinguish between the retinal motion of the moving object and motion patterns generated from the forward translation (Warren & Rushton, 2007). The *flow parsing hypothesis* states that, in order to accomplish this distinction, the brain first parses retinal information of scene-relative object motion from retinal self-motion patterns known as *optic flow*. The brain then performs a subtraction on optic flow and a corresponding subtraction on the retinal motion trajectory. The second subtraction occurs because optic flow alters the object motion trajectory on the retina; the subtraction aims to account for this displacement (Figure 1).
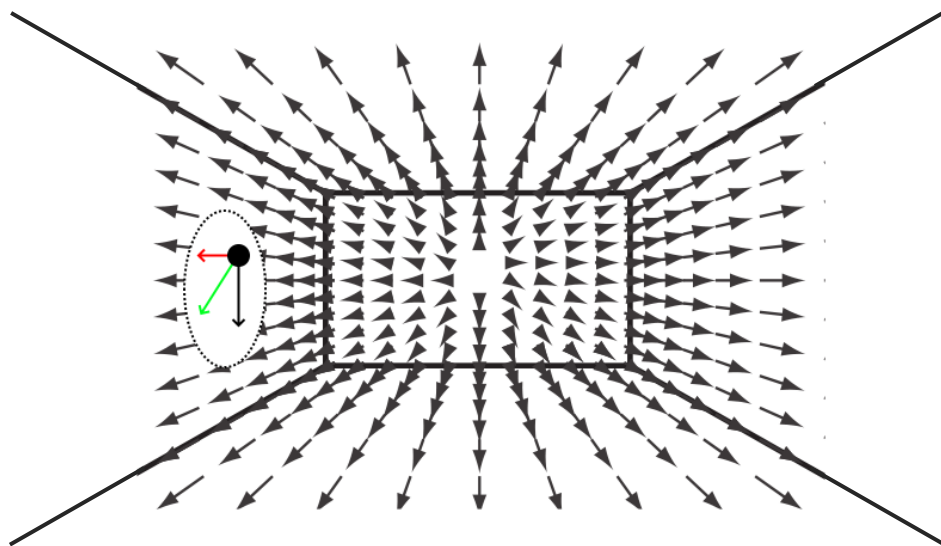

Figure 1. Schematic of inferred retinal self-motion (optic flow) and retinal motion of a moving object (black dot). The red arrow represents inferred optic flow, which is parsed from the retinal motion of the object in green. The final percept is a vertically falling object, as represented by the black arrow.

Evidence of flow parsing is well-documented, as are context-dependent factors like object eccentricity and amount of optic flow information present (Warren & Rushton, 2009). Earlier works in visual perception detail numerous differences in visual processing between the upper and lower visual fields, including the fact that optic flow in the lower visual hemifield induces a greater sense of self-motion, which may be motivated by evolutionary factors (Previc, 1990, Fujimoto & Ashida, 2019). Taken together, these findings raise the following questions: whether

the effects of flow parsing vary depending on the location of optic flow, and whether the location of moving object's retinal motion affect the size of flow parsing.

In the present study, we hypothesized that optic flow located in the lower visual hemifield would have a significantly greater effect on flow parsing as compared to optic flow located in the upper visual hemifield when controlling for the moving object's location. Further, we hypothesize that objects located in the upper visual hemifield will experience a greater global subtraction as compared to objects in the lower visual hemifield when controlling for optic flow location. In order to test these hypotheses, we devised conditions which manipulate object (probe) location, optic flow location or both in order to find the respective contributions of each to flow parsing.

Methods

Subjects

6 naïve undergraduate students at the University of Rochester were recruited for the study. Each subject was over 18 years old and had normal or corrected-to normal vision. The research protocols were approved by the University of Rochester Research Subjects Review Board (RSRB), and informed consent was obtained from all subjects. Subjects were compensated for their time with $20 per session (1.5 hours/session). Each subject except for Subject 1 participated in 3 experimental sessions and performed between 500 and 750 trials per session. Subject 1 was excluded from analyses.

Setup

Experiments were conducted in dark room in a psychophysics lab. A 27-inch monitor was placed 57 cm away from the subject. The subject sat at eye level with the center of the display, ensured by a chinrest and eye tracking software. The experimenters sat in a separate control room from which they could load the stimuli onto the monitor, control lighting, record trial information, and actively monitor the subject's gaze. During each trial, a fixation cross appeared for 1 second at the center of the display, and subjects were instructed to focus on the cross for the duration of the experiment. Then, the fixation cross was replaced by one of 8 conditions presented for 2 seconds. Afterwards, an adjustable dial appeared, and subjects were instructed to adjust to match the probe trajectory they perceived using a keypad.

Visual stimulus

The stimulus was created using the Unity 3D Engine. The camera had a field of view of 90 degrees horizontally and 60 degrees vertically, which moves to generate an expanding view. The speed of forward motion was 100 cm/s. An optic flow field was generated as a virtual cloud of 5000 white spheres with diameter 1 cm presented against a black background. The spheres were

randomly distributed on the depth (z) plane ranging between 0 and 50 meters from the camera, spawning up to 10 meters from the center on both the horizontal (x) plane and vertical (y) plane. A clipping plane was used to only display the spheres that are 2 to 20 meters from the camera; therefore, around 1800 spheres were present to the observers at any given time. The scene was subtended 33.6 cm in height and 59.8 cm in width on the display.

A moving probe was presented either in the upper or lower hemifield along the vertical meridian with a moving trajectory starting at 0.7 m from the center of display. The probe was 2 meters away from the observer at all times. The probe had a linear speed of 10 cm/s, and its direction of movement was coded by the angle between the probe trajectory and the horizontal axis, increasing in counterclockwise direction. The probe's direction of movement was randomly selected from one of ten sectors of 36 degrees across the full 360 range.

To explore whether flow field location imposes an effect on the perception of object movement during ego movement, we designed 8 conditions varying across four flow field locations and two probe locations as shown in Figure 2.
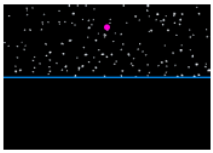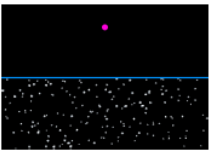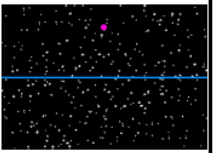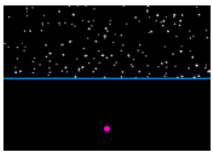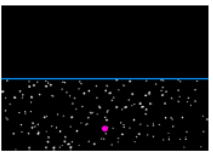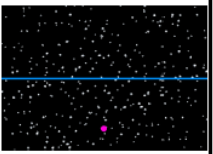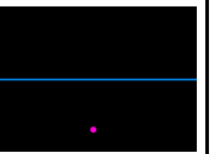

	Flow at top	Flow at bottom	Full Flow	No Flow
Probe at top	$F_{Top}P_{Top}$	$F_{Bottom}P_{Top}$	$F_{Full}P_{Top}$	$F_{Control}P_{Top}$
Probe at bottom	$F_{Top}P_{Bottom}$	$F_{Bottom}P_{Bottom}$	$F_{Full}P_{Bottom}$	$F_{Control}P_{Bottom}$

Figure 2. Schematic illustrations of the experimental and baseline conditions. The four columns correspond to four flow field conditions, and the two rows indicate two probe locations in each flow field condition. The terms under the illustrations are the abbreviation of condition names, which will be used throughout the paper. F denotes optic flow, and P denotes probe. The subscripts under F indicate the optic flow condition. The subscripts under P indicate the location of the probe in each condition. For example, $F_{Top}P_{Bottom}$ denotes optic flow being in the upper hemifield and probe in the lower hemifield.

The Control condition serves as a baseline that measures subjects' ability to accurately judge the probe direction in the absence of optic flow using a virtual dial, with the probe presented either at

the upper or lower hemifield. The Full condition contains optic flow across the entire visual scene, with the probe appearing either in the upper or lower hemifield. This allows us to measure the following components of flow parsing:

1. the global effect of top and bottom optic flow on the inference of self-motion
2. the global effect of inferred self-motion on the estimation of object motion at top / bottom
3. the local effect of optic flow on the estimation of object motion at top / bottom

We refer to the effects in 1 as G_{self}^{top} and G_{self}^{bot}, the effects in 2 as G_{obj}^{top} and G_{obj}^{bot}, and the effects in 3 as L_{obj}^{top} and L_{obj}^{bot}. The capital letters G and L denote the global or local mechanism contributing to the effect. The superscripts top and bot denote the upper and lower hemifields in which the mechanism is used. The subscripts $self$ and obj denote the target on which the mechanism acts (i.e., self-motion or the moving object). A conceptual diagram of the components of flow parsing is illustrated in Figure 3.

The flow at bottom (F_{Bottom}) condition presents optic flow within only the lower hemifield, while the flow at top (F_{Top}) condition presents optic flow within only the upper hemifield. Probe location varies across top and bottom in either flow field conditions.
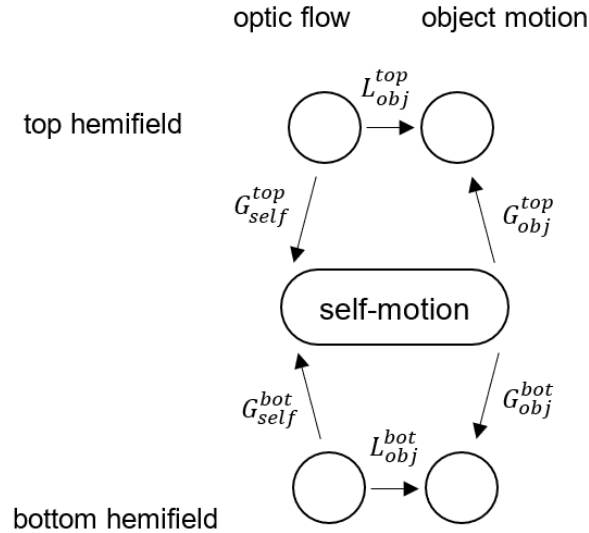
Figure 3. Conceptual diagram of the components of flow parsing. The circles represent the source or target of effects, and the arrows denote the inference process underlying the effects. In the top half of the diagram, when the object is in the upper hemifield, optic flow in the upper hemifield exerts a global effect on the inference of self-motion (G_{self}^{top}) and local effect on the estimation of object motion (L_{obj}^{top}) at that location. The inferred self-motion then has a global effect acting on the object (G_{obj}^{top}) to help with the estimation of object motion. The same process applies to the object being in the lower hemifield.

Data Analysis

Flow parsing gain

To quantify the bias produced by optic flow, we computed the *flow parsing gain* using the following equation:

$$\alpha = \sum_{i=1}^{n} \left(\theta_r^i - \arctan \frac{v_y^i - \alpha\, u_y^i}{v_x^i - \alpha\, u_x^i} \right)^2$$

where α is flow parsing gain, θ is the direction reported by the subjects, v_x and v_y are the probe velocity in the horizontal and vertical directions, and u_x and u_y are the optic flow velocity in the horizontal and vertical directions, respectively.

A full subtraction of the optic flow vector is represented by gain $= 1$, while gain $= 0$ represents no subtraction happening at the location of the probe. Partial subtraction with a gain between 0 and 1 is expected for all conditions.

Linear model

In order to tease out the contributions by the probe and optic flow on upper and lower hemifields, we devised a set of equations to account for the contributions of various local and global mechanisms by using linear combinations of the six variables L_{obj}^{top}, L_{obj}^{bot}, G_{self}^{top}, G_{self}^{bot}, G_{obj}^{top}, and G_{obj}^{bot}. A schematic of the equations describing the composition of local and global contributions for each condition are shown in Table 1. We utilized this system of equations to isolate the six sources of contribution on flow parsing by subtracting one equation from another.

Conditions			Gain			
Abbr.	**Optic flow**	**Object**	*Resulting from a combination of local and global contributions*			
$F_{Full}P_{Top}$	Full	Top	L_{obj}^{top} +	G_{self}^{top} +	G_{self}^{bot} +	G_{obj}^{top}
$F_{Full}P_{Bottom}$	Full	Bottom	L_{obj}^{bot} +	G_{self}^{top} +	G_{self}^{bot} +	G_{obj}^{bot}
$F_{Top}P_{Top}$	Top	Top	L_{obj}^{top} +	G_{self}^{top} +	+	G_{obj}^{top}
$F_{Top}P_{Bottom}$	Top	Bottom	+	G_{self}^{top} +	+	G_{obj}^{bot}
$F_{Bottom}P_{Top}$	Bottom	Top			G_{self}^{bot} +	G_{obj}^{top}
$F_{Bottom}P_{Bottom}$	Bottom	Bottom	L_{obj}^{bot} +		+ G_{self}^{bot} +	G_{obj}^{bot}

Table 1. Linear combinations of local and global contributions for each unique condition. All statistical analyses were performed using R.

Results

We hypothesized that the flow parsing effect would be stronger when optic flow is in the lower visual hemifield, and that it would exhibit no difference with respect to object location in the vertical hemifields. To quantify the relative effects of flow parsing, we calculated *flow parsing gain*, which measures the amount of optic flow a subject subtracts from object motion. We obtain flow parsing gain α by finding a value that would minimize the sum of squared differences between subject's perceived probe angle and the expected probe angle if maximum flow parsing were to occur.

Using the mathematical model described above, we fit each subject's data to the prediction results. Figure 4A shows a comparison across all unique flow and probe locations for one of the subjects. For the $F_{Top}P_{Top}$ condition and both of the F_{Full} conditions, the subject's data appears to systematically deviate from the model prediction in being closer to the diagonal when the probe is moving perpendicular to the optic flow at 90° (rightward) and 270° (leftward). A qualitative discrepancy in how the model prediction and subject data deviate from the $y = x$ line suggests a need to further refine the model we used to calculate flow parsing gain.
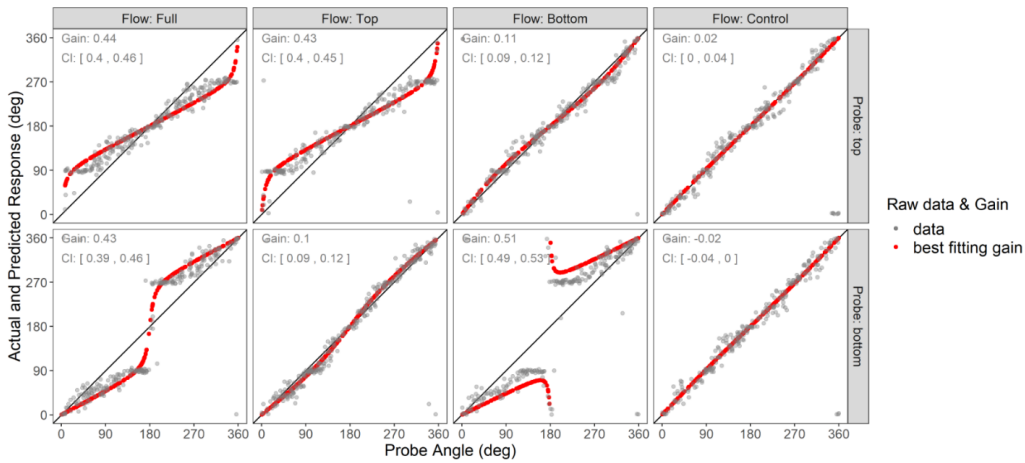

Figure 4A. Comparison between perceived and actual direction of probe motion for one of the subjects ($N = 1$) across all eight unique conditions. The gray points are the subject's raw data while the red curve is the predicted subject response, calculated with the best-fitting gain. The top left corner indicates the best-fitting gain and the bootstrapped 95% confidence interval.

Figure 4B shows perceived and actual probe directions of motion for the same subject as in Figure 4A for the Full optic flow condition when the probe moves in the upper hemifield. The plots for flow parsing gain = 0 and flow parsing gain = 1 are plotted for reference. A gain of zero would imply that a subject did not perform flow parsing at all, while a gain of one would

imply that a subject performed the largest possible amount of flow parsing given the information present in the visual field. As expected, the predicted curve for the subject's calculated gain of 0.44 lies between the curves with maximum and minimum gain, showing partial flow parsing.
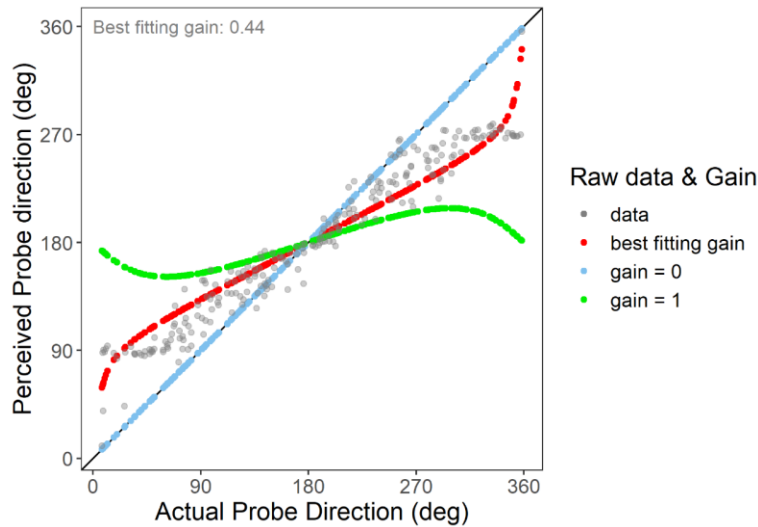

Figure 4B. Comparison between perceived and actual direction of probe motion for the same subject ($N = 1$) for the $F_{Full}P_{Top}$ condition. The gray points are the subject's raw data; the blue curve represents what the subject's data would look like with minimum flow parsing; the green curve represents what the data would look like with maximum flow parsing. As expected, the subject's predicted curve using best-fitting gain lies between gain $= 0$ and gain $= 1$.

Next, we compared across all subjects ($N = 6$) under different conditions by comparing each of their flow parsing gains across 1000 bootstrapped trials. Figure 5A shows that, in the Full conditions, all subjects produce flow parsing gains that are statistically significant from zero. This is consistent with our expectations, as there is optic flow across the entire visual field; hence, subjects should subtract the largest amount of optic flow from the moving probe in the Full conditions. Moreover, half of the subjects do not show a statistically significant difference between the vertical hemifields, while the other half exhibits a stronger effect when the probe moves in the upper hemifield. Figure 5B shows that, in the Control condition, more than half of the subjects' data points are significantly different from gain $= 0$ on both axes. This result deviates from our expectation (i.e., that all flow parsing gains in the Control condition should not be significantly different from zero), and raises an important question of what may have caused the deviation from gain $= 0$. Furthermore, four of the six subjects have gains that lie above the $y = x$ line, suggesting a flow parsing bias toward the upper hemifield based on probe location. In other words, in the absence of optic flow in the stimulus, subjects still perceived a certain amount of optic flow and subtracted the vectors from probe motion when it moved in the upper visual hemifield. The fact that certain data points deviate from the gain $= 0$ lines and lie above

the $y = x$ lines suggests that, for the following comparisons we make across various experimental conditions, any inference we make from our data needs to account for the possibility of underlying individual differences.
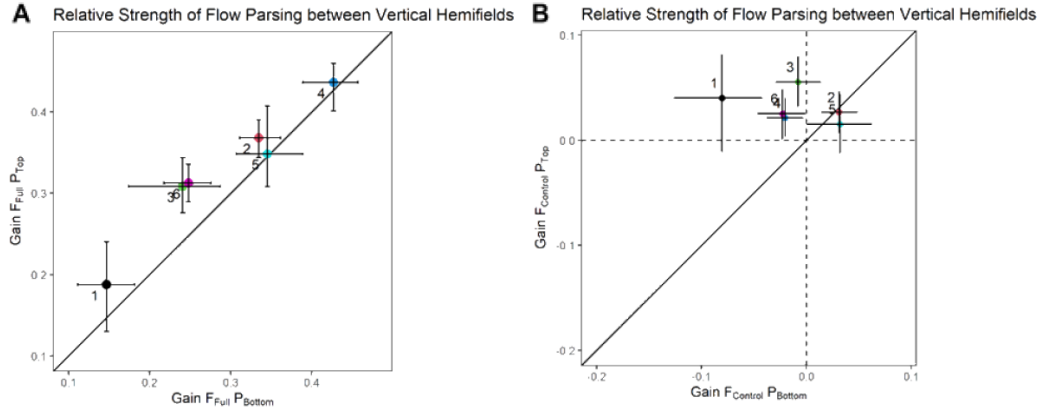

Figure 5. Comparison of bootstrapped flow parsing gain between vertical hemifields, averaged across each of six subjects ($N = 6$). Each subject is labeled by a number next to the corresponding averaged bootstrapped gain. Error bars represent 95% confidence intervals. The diagonal line ($y = x$) represents no difference in flow parsing gain between conditions labeled on the x and y axes. **(A)** Comparison between the $F_{Full}P_{Top}$ and $F_{Full}P_{Bottom}$ conditions. **(B)** Comparison between the $F_{Control}P_{Top}$ and $F_{Control}P_{Bottom}$ conditions. The dotted lines indicate gain $= 0$ when the probe moves in the upper and lower hemifields, respectively.

The plots for the Full and Control conditions in Figure 5 show what would have yielded maximum and minimum flow parsing, respectively. To make more extensive comparisons, we first compare subjects' flow parsing gains when the probe was moving in the same or opposite hemifield as the optic flow in the vertical visual hemifields. In Figure 6A, we see that nearly all subjects demonstrated a stronger flow parsing effect when the optic flow and probe are in the same hemifield – except for Subject 3 in the $F_{Bottom}P_{Bottom}$ condition, in which the confidence interval slightly overlaps with the $y = x$ line. The fact that subjects produced stronger flow parsing gain when optic flow and probe are in the same hemifield is consistent with our expectation. As shown by Figure 3, when both the optic flow and the probe are in the same vertical hemifield, both local and global factors contribute to flow parsing; when the optic flow and the probe are in opposite hemifields, local factors are absent and only global contributions remain. Since there are more sources of contribution to the flow parsing effect in the former case, a greater degree of flow parsing gain is expected and observed in our data.

Next, we attempt to tease out the contributions of probe motion on optic flow by comparing the conditions in which the optic flow and probe lie in opposite vertical hemifields. In these conditions, local contributions immediately surrounding the probe are completely removed, so

any flow parsing effect we observe would be due to global mechanisms. In Figure 6B, half of the subjects display no difference between when the optic flow is present in the upper or lower visual hemifield, while the other half exhibits stronger flow parsing effect then optic flow is in the lower hemifield. Our data appears to be consistent with our first hypothesis, i.e., optic flow in the lower visual hemifield exerts a stronger effect on flow parsing than that in the upper visual hemifield. However, it is important to note that Figure 6B is confounded by probe location, so despite removing local information completely, we still cannot distinguish whether the significant effects should be attributed to optic flow or probe location. Hence, we cannot yet conclude that optic flow in the lower visual hemifield produces a stronger flow parsing effect.
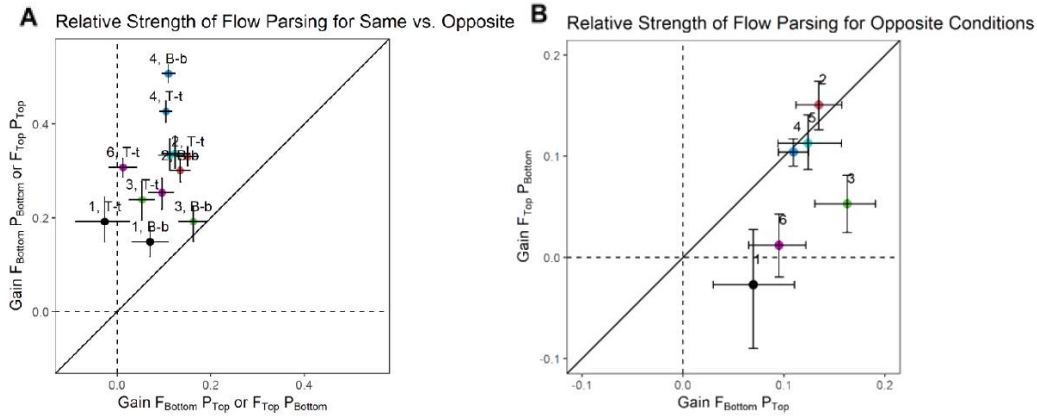

Figure 6. Comparison of bootstrapped flow parsing gain, averaged across each of six subjects ($N = 6$). Each subject is labeled by a number next to the corresponding averaged bootstrapped gain. Error bars represent 95% confidence intervals. The diagonal line ($y = x$) represents no difference between values on the x and y axes. Dotted lines indicate gain $= 0$. **(A)** Comparison between conditions when the optic flow and probe are in the same vs. opposite vertical hemifields. **(B)** Comparison between the $F_{Top}P_{Bottom}$ and $F_{Bottom}P_{Top}$ conditions.

In order to isolate the effects of local and global contributions to flow parsing, we utilized the linear equations in the schematic in Table 1 by performing subtractions to solve for L_{obj}, G_{obj} and G_{self}, respectively. The calculations for each variable are shown below and continue on the following page.

We obtain L_{obj} by performing the following linear operations:

Equation 1: $F_{Full}P_{Top} - F_{Bottom}P_{Top}$

$$\left(L_{obj}^{top} + G_{self}^{top} + G_{self}^{bot} + G_{obj}^{top}\right) - \left(G_{self}^{bot} + G_{obj}^{top}\right) = L_{obj}^{top} + G_{self}^{top}$$

Equation 2: $F_{Full}P_{Bottom} - F_{Bottom}P_{Bottom}$

$$\left(L_{obj}^{bot} + G_{self}^{top} + G_{self}^{bot} + G_{obj}^{bot}\right) - \left(L_{obj}^{bot} + G_{self}^{bot} + G_{obj}^{bot}\right) = G_{self}^{top}$$

Equation 3:   Equation 1 – Equation 2

$$\left(L_{obj}^{top} + G_{self}^{top}\right) - \left(G_{self}^{top}\right) = \boxed{L_{obj}^{top}}$$

Equation 4: $F_{Full}P_{Bottom} - F_{Top}P_{Bottom}$

$$\left(L_{obj}^{bot} + G_{self}^{top} + G_{self}^{bot} + G_{obj}^{bot}\right) - \left(G_{self}^{top} + G_{obj}^{bot}\right) = L_{obj}^{bot} + G_{self}^{bot}$$

Equation 5: $F_{Full}P_{Top} - F_{Top}P_{Top}$

$$\left(L_{obj}^{top} + G_{self}^{top} + G_{self}^{bot} + G_{obj}^{top}\right) - \left(L_{obj}^{top} + G_{self}^{top} + G_{obj}^{top}\right) = G_{self}^{bot}$$

Equation 6:   Equation 4 – Equation 5

$$\left(L_{obj}^{obj} + G_{self}^{bot}\right) - \left(G_{self}^{bot}\right) = \boxed{L_{obj}^{bot}}$$

We obtain G_{self} by performing the following linear operations:

Equation 7: $F_{Full}P_{Bottom} - F_{Bottom}P_{Bottom}$

$$\left(L_{obj}^{bot} + G_{self}^{top} + G_{self}^{bot} + G_{obj}^{bot}\right) - \left(L_{obj}^{bot} + G_{self}^{bot} + G_{obj}^{bot}\right) = \boxed{G_{self}^{top}}$$

Equation 8: $F_{Full}P_{Top} - F_{Top}P_{Top}$

$$\left(L_{obj}^{top} + G_{self}^{top} + G_{self}^{bot} + G_{obj}^{top}\right) - \left(L_{obj}^{top} + G_{self}^{top} + G_{obj}^{top}\right) = \boxed{G_{self}^{bot}}$$

We obtain G_{obj} by performing the following linear operations:

Equation 9: $F_{Top}P_{Bottom} - G_{self}^{top}$

$$\left(G_{self}^{top} + G_{obj}^{bot}\right) - \text{Equation 7} = \boxed{G_{obj}^{bot}}$$

Equation 10: $F_{Bottom}P_{Top} - G_{self}^{bot}$

$$\left(G_{self}^{bot} + G_{obj}^{top}\right) - \text{Equation 8} = \boxed{G_{obj}^{top}}$$

The results of the linear subtractions are shown in Figure 7. We examined the comparison between G_{self}^{bot} and G_{self}^{bot} (Figure 7A) and G_{self}^{bot} and G_{self}^{bot} (Figure 7B). In both figures, all subjects except for Subject 4 do not show a statistically significant effect toward the upper or lower hemifield. In Figure 7C, a comparison between L_{obj}^{top} and L_{obj}^{bot} suggests that, again, only Subject 4 demonstrates a statistically significant effect toward the upper hemifield. The rest of the subjects do not show a stronger effect of flow parsing due to local mechanisms in either of the vertical visual hemifields. After isolating the different local and global contributions on flow parsing using the schematic in Figure 3, we obtain a result that is contrary to what Figure 6B suggests – that there is no significantly stronger flow parsing effect when optic flow is in the lower hemifield.
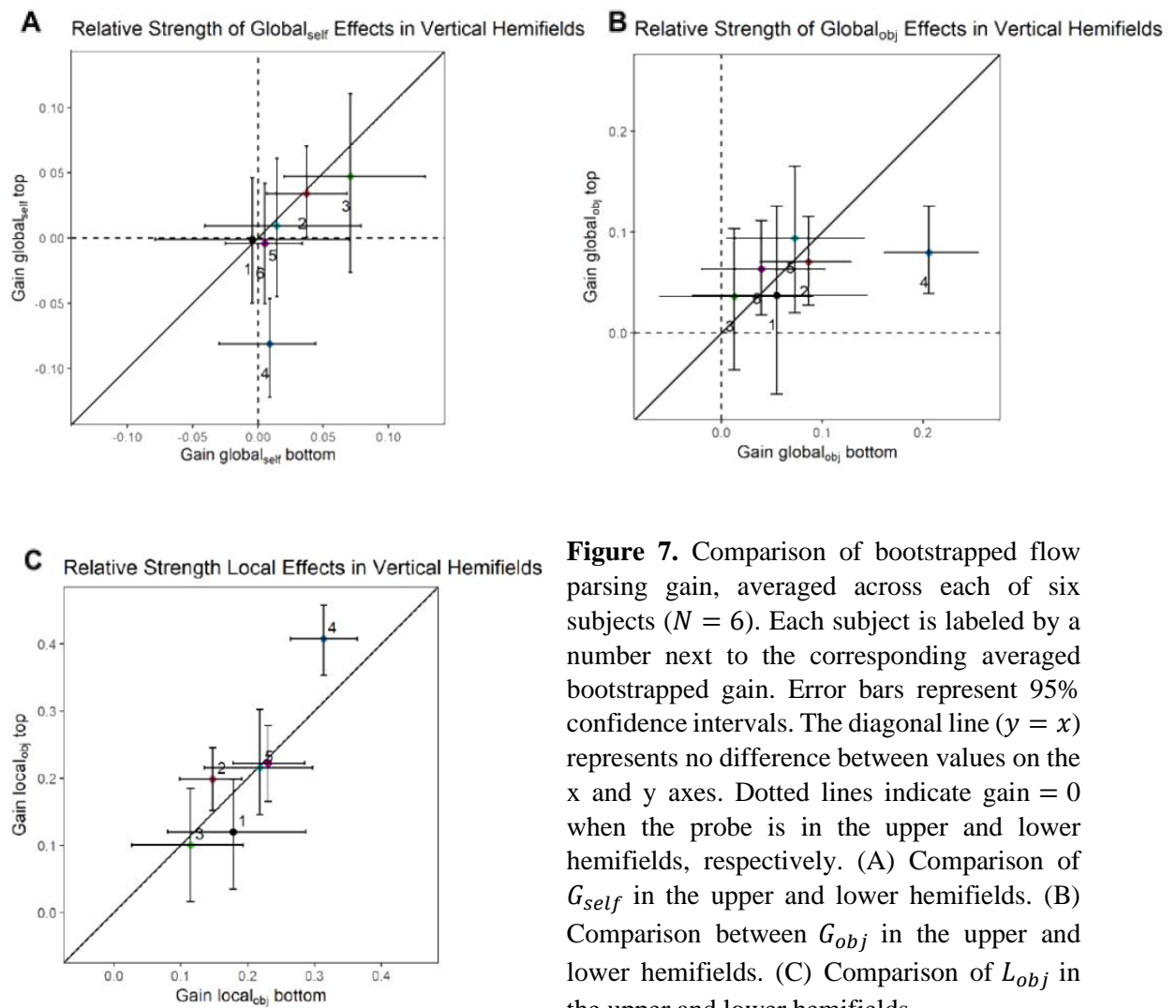

Figure 7. Comparison of bootstrapped flow parsing gain, averaged across each of six subjects ($N = 6$). Each subject is labeled by a number next to the corresponding averaged bootstrapped gain. Error bars represent 95% confidence intervals. The diagonal line ($y = x$) represents no difference between values on the x and y axes. Dotted lines indicate gain $= 0$ when the probe is in the upper and lower hemifields, respectively. (A) Comparison of G_{self} in the upper and lower hemifields. (B) Comparison between G_{obj} in the upper and lower hemifields. (C) Comparison of L_{obj} in the upper and lower hemifields.

Discussion

Differences between the upper and lower visual fields have long been documented in literature for various visual tasks. Previous works seem to converge on the same set of observations: that the upper visual hemifield seems to be more sensitive to more local information, while the lower visual hemifield seems to be attuned to global information. However, the implications of the human brain's sensitivity to a particular vertical hemifield have yet to be investigated. In this study, we examined the relationship between global and local mechanisms of optic flow processing in the upper and lower visual hemifields. We proposed the following hypotheses: 1) global flow parsing gain would be stronger in the lower visual hemifield compared to the upper hemifield; and 2) local flow parsing gain would be stronger in the upper visual hemifield compared to the lower hemifield.

Contrary to our hypotheses, our results demonstrated no significant difference between the upper and lower visual hemifields. Aside from a single subject, who neatly slotted into our proposed hypotheses, we were unable to determine if either global or local flow parsing gain was stronger in one hemifield versus the other for any of the other subjects due to confounding factors.

Related Work

Previc (1990)

The key finding of Previc (1990) was that our upper and lower visual hemifields were specialized to serve different functions. We used such findings as a motivation for our current study, particularly evidence that the lower visual hemifield is specialized for global processing, e.g., stereo-motion, while the upper visual hemifield is specialized for local processing, e.g., object perception. Our results partially support previous findings, such that one of the subjects showed more global flow parsing gain in the lower visual hemifield, and more local flow parsing gain in the upper visual hemifield. However, no such conclusions could be made for the rest of the subjects.

Fujimoto & Ashida (2019)

At cursory glance, it may seem that our findings are at odds with the study conducted by Fujimoto & Ashida (2019), whose findings suggest that a greater sense of self-motion is induced by optic flow in the lower hemifield when compared to optic flow in the upper hemifield. In our linear model, G_{self} represented the global component of flow parsing gain that was derived from the effect of optic flow on our sensation of self-motion. This component, as shown in Figure 7A, is essentially the same component that was investigated by Fujimoto and Ashida (2019). Since flow parsing is dependent on an inference of self-motion from optic flow, in order to be

compatible with Fujimoto and Ashida (2019), our observations would have to demonstrate greater flow parsing gain in the lower hemifield when compared to the upper hemifield. However, this was not the case, as we were unable to suggest that a difference exists in flow parsing gain between the two visual hemifields.

Warren and Rushton (2009)

The two principal findings from Warren and Rushton (2009), in the context of the current study, were that 1) global mechanisms are implicated in the flow parsing process; and that 2) global mechanisms can operate in the absence of local information. Our findings were largely consistent with these observations.

What's important to note about Figure 7A and B is that it does not implicate any local mechanisms. Hence, Figure 7 is consistent with the findings of Warren and Rushton (2009) that a global mechanism exists for scene-relative object motion estimation during forward translation. This effect is also apparent in conditions where the object was in a separate hemifield from the optic flow. In the complete absence of local optic flow information, a degree of flow parsing gain was still observed, suggesting that this global mechanism can also operate in the absence of local information.

Our findings differed from that of Warren and Rushton (2009) in that we were unable to discount the importance of a local mechanism for optic flow. Figure 6A demonstrates that flow parsing gain is significantly mitigated when the probe moves in the hemifield that is opposite of the optic flow (i.e., no local information). Furthermore, Figure 7C demonstrates that a significant amount of flow parsing gain is derived from local information. Hence, it is possible that both global and local mechanisms contribute to our perception of independently moving objects during self-motion in a significant manner.

Prior to the current study, we conducted a replication study of Warren and Rushton (2009). A novel observation we made from our replication results was that optic flow information in one hemifield did not seem to affect flow parsing in the other. We had two explanations for this observation. First, it is possible that optic flow information does not transfer between lateral visual hemifields. Second, it could be that global mechanisms cannot act in the absence of local information. Since our results showed that a global mechanism persists in the absence of local information, the second explanation can be discounted. In other words, we have reason to believe that optic flow information does not transfer between lateral visual hemifields, but we believe that this observation is likely a result of problems inherent to our original study. Therefore, further investigation into this phenomenon would help to elucidate potential flaws in our original study.

Limitations

Our study has several limitations. While we expanded upon our corpus of information compared to our previous studies, we lacked the statistical power to make several key differentiations. For example, in Figure 5A, which shows the differences in flow parsing gain between the upper and lower visual hemifields, only one subject clearly deviates from the diagonal, demonstrating a difference in flow parsing gain between the two vertical hemifields. While the other five subjects also seem to lie on the same side of the diagonal, the large sizes of the error bars prevent us from drawing the same conclusion as the former subject.

Furthermore, even though we closely monitored all subjects with an eye tracking device throughout the duration of all trials and instructed participants to focus on the center of the screen, we did not strictly prohibit eye movements of the observers. As such, our data is reflective of an experimental paradigm in which there is a lack of controlled eye-movements. This is problematic because, hypothetically speaking, if the subject focuses his or her eyes on the probe even as it moves, then the moving probe will always occupy the center of the retina under all conditions, potentially nullifying any effect from the probe or optic flow location we would expect to see in a particular condition.

Another limitation of our study is that the stimulus – a standard radial dot field display – we presented to the recruited subjects is unrepresentative of actual environments that the human visual system is optimized for. We will discuss this as a potential future direction in Conclusion.

Conclusion

Based on our observations from the current study, neither global nor local mechanisms contribute to significantly greater flow parsing gain in vertical visual hemifield. It might be possible that, while our vertical visual fields are specialized for different functions and attuned to different types of information, flow parsing remains relatively unaffected by this disparity. Future studies should increase the sample size with a goal of increasing statistical power, enforce a stricter requirement for fixating on the center of the display, as well as refining our stimulus to represent a naturalistic scene instead of using a virtual cloud of white spheres to simulate forward motion. It is crucial to address these limitations before further conclusions can be drawn from the results.

References

[1] Fujimoto, K., & Ashida, H. (2019). Larger Head Displacement to Optic Flow Presented in the Lower Visual Field. *I-Perception*.

[2] Gogel, W.C., and Koslow, M. (1972). The adjacency principle and induced movement. *Perception & Psychophysics*, 11, 309–314.

[3] Niehorster, D. C., & Li, L. (2017). Accuracy and Tuning of Flow Parsing for Visual Perception of Object Motion During Self-Motion. *I-Perception*.

[4] Previc, F. H. (1990). Functional specialization in the lower and upper visual fields in humans: Its ecological origins and neurophysiological implications. *The Behavioral and Brain Sciences*, *13*(3), 519-542.

[5] Warren, P. A., & Rushton, S. K. (2008). Evidence for Flow-Parsing in Radial Flow Displays. *Vision Research*, 48, 655–663.

[6] Warren, P. A., & Rushton, S. K. (2009). Optic Flow Processing for the Assessment of Object Movement during Ego Movement. *Current Biology*, 19(18), 1555–1560.

[7] Warren, W.H., & Hannon, D.J. (1988). Direction of self-motion is perceived from optical flow. *Nature*, 336, 162–168.